Segmenting/Pre-Processing Data from Bone Screw Thread-Stripping Tests

Jack Wilkie[1,2], Nour Aldeen Jalal[1], Georg Rauter[2], and Knut Möller[1,3,4]

***Abstract*— Bone screws must be appropriately tightened to achieve optimal patient outcomes. If over-torqued, the threads formed in the bone may break, compromising the strength of the fixation; and, if under-torqued, the screw may loosen over time, compromising the stability. Previous work has proposed a model-based system to automatically determine the optimal insertion torque. This system consists of a reverse-modelling step to determine strength, and a forward modelling step to determine maximum torque. These have previously been tested in isolation, however future work must test the combined system. To do so, the data must be segmented and pre-processed. This was done based on specific features of the recorded data. The methodology was tested on 50 screw-insertion data sets across 5 different materials. With the parameters used, all data sets were correctly segmented. This will form a basis for the further processing of the data and validating the combined system**

***Clinical relevance:* The system for torque limit determination must be tested in its entirety to properly asses its performance. This paper discusses some of the steps required to pre-process the data to make this assessment. If successful, this system may improve patient outcomes in orthopaedic surgery.**

I. Introduction

Bone screws are used in orthopaedic surgery to fix bone in place and assist natural healing of traumatic fractures, or to secure implants that may improve the quality-of-life of previously disabled people. In either case, the strength and longevity of the fixation is important to achieve the best patient outcomes. The torque that is used to tighten the screw can be an important factor affecting this strength and longevity. If under-torqued, the screw may loosen over time, leading to instability [1]. And, if over-tightened, the threads formed in the bone may break, compromising the strength of the fixation [2]. Both situations may necessitate revision surgery, which is costly in both the financial sense, and in terms of addition risks to the patient.

In current surgical practice, screws are normally tightened *ad-hoc*, with the surgeon relying on experience and tactile feedback to determine when the screw is appropriately tight. While this often achieves good outcomes, errors still occur[3], as it is a subjective process, and may be impacted by human factors like fatigue and stress. Furthermore, not all surgeons have the same level of skill and/or experience. Hence, developing some system to objectively determine the appropriate tightness may lead to better patient outcomes.

In previous work, a system has been proposed to achieve this goal of automatic torque limit determination. This system involved determining the strength of the material based on the torque-rotation profile of the screw insertion [4], [5], then using this with a forward model to predict stripping torque [6]. While these aspects have been tested separately [6], [7], thorough testing and characterisation of the complete system remains.

The planned procedure for the full model testing is to insert a screw into a test material completely until the threads strip. This gives a ground-truth value for the stripping torque, and the above method can be applied to data prior this stripping to obtain the estimated value for comparison. This paper documents the pre-processing procedure for the screw insertion data. This includes correcting any offsets in the raw data, trimming the data to relevant time period, and performing any required unit conversions. It also discusses the relevance of this and the required modifications for use in a real-time system.

II. Methods

A. Data Collection

The data was collected using a purpose-built test rig for screw insertion testing, shown in Fig. 1. This used a closed-loop controlled stepper motor to insert the screw at a fixed angular velocity (34HS46-6004D-E100, OMC Corporation Limited). During insertion, the torque, position, and rotation were measured at 1000 Hz. An NCTE-2300-5-1-AU-0-0 (NCTE AG) rotational torque sensor was used for the torque and rotation, and an A40/D5.2501.2421.1000 (Fritz Kübler GmbH) draw-wire encoder was used for the linear position.

A 30 mm-long HB 6.5 bone screw (ISO 5835:1991 [8]) was fully screwed into a pre-drilled polyurethane foam block at 30 RPM, until the threads stripped. A block of SikaBlock M600 (Sika Deutschland AG) rigid polyurethane foam material was used as a synthetic substitute for real bone due to its similar properties [9], and it is also often used for training models [10], [11]. The properties of this PU foam (0.60 g/cc Density, 16-18 MPa Strength, and 750 MPa Youngs modulus [12]) are in the range of cancellous bone (0.61-0.88 g/cc Density, 0.15-21 MPa Strength, and 345-1475 MPa Youngs modulus [13], [14]) The position of the screw was zeroed where the tip of the screw first crosses the plane representing the surface of the test block.

*This work was partially supported by grants "CiD" and "Digitalisation in the OR" from BMBF (Project numbers 13FH5E02IA and 13FH5I05IA).

[1]Jack Wilkie, Nour Aldeen Jalal, and Knut Möller are with the Institute for Technical Medicine (ITeM), Hochschule Furtwangen, Jakob-Kienzle-Straße 17, Villingen-Schwenningen, Germany wij@hs-furtwangen.de

[2]Jack Wilkie and Georg Rauter are also with the BIROMED-Lab, Department of Biomedical Engineering, University of Basel, Basel, Switzerland

[3]Knut Möller is also with the Centre for Bioengineering, University of Canterbury, 20 Kirkwood Avenue, Christchurch, New Zealand

[4]Knut Möller is also with the Department of Microsystems Engineering, University of Freiburg, Georges-Köhler-Allee 102, Freiburg, Germany

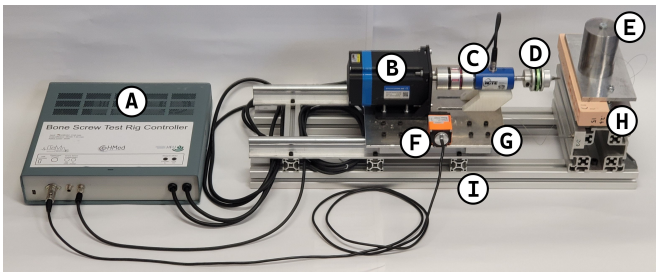

Fig. 1. Test rig for bone screw insertion. A: Control box. B: Motor. C: Torque sensor. D: Screwdriver tip. E: Weight. F: Draw-wire encoder. G: Sliding carriage. H: Sample Clamp. I: Base of test rig.

B. Data Processing

The data recording can be split into 8 distinct sections, denoted *A* to *I* as shown in Fig. 2. *A* represents the steady-state prior to starting insertion. *B* represents when the motor start to insert the screw, but the threads are not fully engaged (note the rotation changing without much change in linear position). *C* represents normal screw insertion where rotational and linear velocity are proportional, this is the most important section for determining the material strength of bone. *D* represents the screw beginning to tighten, with maximum torque achieved at the threshold between sections *D* and *E*. In section *E* the threads cut into the hole are being stripped out, and the torque reduces as the material breaks; at this point the screw rotates without advancing further. In section *E* the insertion stops for a short pause. Section *G* is the screw being unscrewed. Section *H* is after the screw has fully reversed but is still rotating. Section *I* is after the test is fully complete but before the recording was stopped.

The transitions between these different sections should be programmatically determinable. However some are simpler to find than others.

The transition from A to B can be detected when the rotational position first starts to increase beyond its initial value (e.g. using a threshold of 0.1 radian). B to C can also be approximated when the position first starts increasing (e.g. using 0.2 mm threshold). The transition from D to E is approximately when the maximum torque is measured (or alternatively when the linear position first reaches its maximum value). E to F is simply when the rotation first reaches its maximum value. F to G is when the rotation is last at its maximum value. G to H is when the position last exceeds first reaches the final minimum. And, H to I is when the rotation last exceeds its final value.

The transition from C to D is slightly more complex, but can be detected by numerically differentiating the Torque signal. With appropriate smoothing, the steeper section can be detected when the derivative exceeds some multiple of some percentile; this can be tuned to adapt it depending on signal and noise strength, however in this case 3 times the 80th percentile was used with a 1000-sample (1 s) moving average filter, as shown in Fig. 3.

The above conditions were implemented in MATLAB R2020a.

The screw position was zeroed as the tip was at the edge of the pre-drilled hole. This allows for a consistent setup, but is not suitable for the models of screw insertion that must be applied, where the zero point is when the threads first touch the whole walls. Because of this, a simple distance correction (Eqn. 1) is applied based on the taper at the end of the screw.

$$x_{\text{offset}} = \frac{D_{\text{hole}}}{2} \tan\left(\frac{\theta_{\text{taper}}}{2}\right) \tag{1}$$

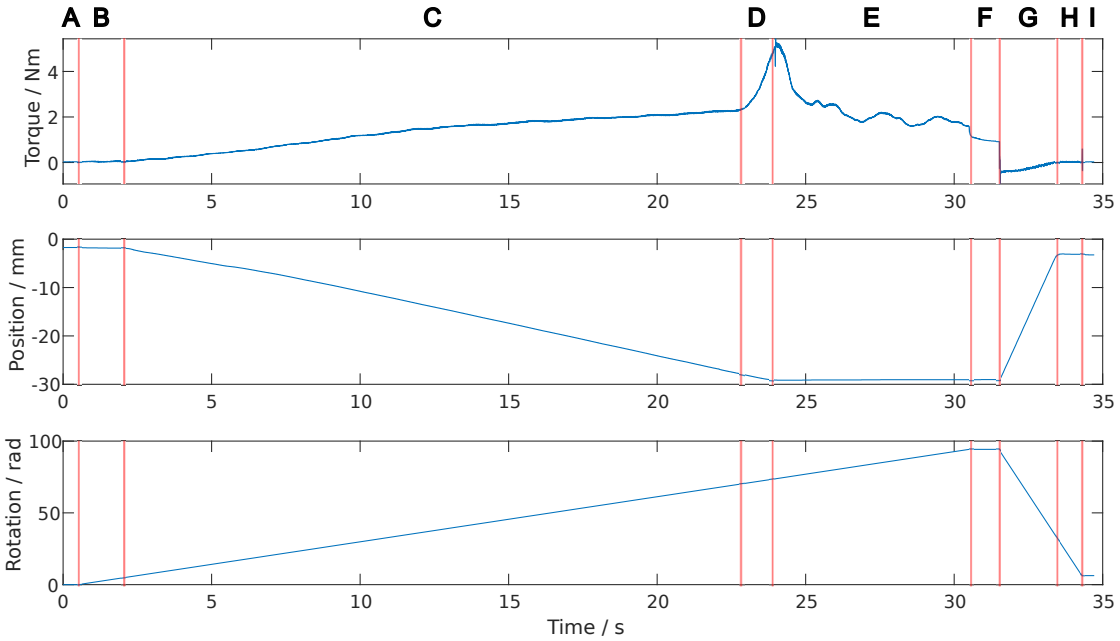

Fig. 2. Phases of screw insertion labelled A-I.

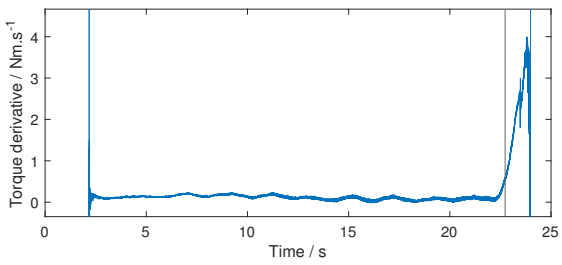

Fig. 3. Phases of screw insertion labelled A-I.

Additionally, the model uses the angular position to measure the depth of the screw, however due to slippage during the initial engagement of the screw in the hole, the rotational values measured by the test rig are not entirely reliable. Therefore, the linear position of the screw is converted into an equivalent angular position based on the pitch of the screw.

To test the segmentation, it was run on the data from 50 insertion tests in 5 different densities of polyurethane foam. All of the results were plotted together with the times rescaled to have matching transition points between the different phases described above.

III. Results

The results of running the segmentation on 50 different datasets are presented in Fig. 4. This also shows a number of clusterings of lines from the different densities of foam tested, showing the different magnitudes for the torque signals.

IV. Discussion

For thoroughly testing the full system of torque limit estimation, the most important aspects of the segmenting are to correctly identify the maximum torque, and to correctly select the period of screw insertion. The relevant section is primarily section C, although in practice data from B and D are available and may provide additional information outside the scope of current modelling. Looking at Fig. 4, The maximum torque limits are correctly identified, and section C goes from when the screw begin to pull itself into the hole, until just before the torque spikes from the tightening, as specified. The other section, while less important for the planned future work, are also correctly segmented.

The methods used here would need some modification to use in a real-time system in a clinical environment. In this case only the transitions between A,B,C, and D are relevant; as ideally anything after stripping would be avoided. However, detecting if the screw was inadvertently stripped (D to E transition) would require some additional logic, as it is not so easy to detect if torque has peaked, since it is not known if it may go higher still; this could be based on quantifying the prominence of the peak. Additionally, in a real system (e.g. with a gyroscope in a handheld screwdriver), the exact zero point is not so clear; this could be detected with more advanced algorithms (e.g. combination of conditions on torque, axial force, and rotation.), or could be simply activated by a button on the screwdriver.

One limitation is that empirical thresholds were used to account for noise that is present in the data (e.g. so that the start of insertion is not prematurely detected due to vibrations). This means that while the segmenting is automated, the results should be manually checked; however this is still a significant time-saving compared with manually completing this task. This was also an issue for detecting the exact torque-derivative threshold for the transition from segment C to D. The initial

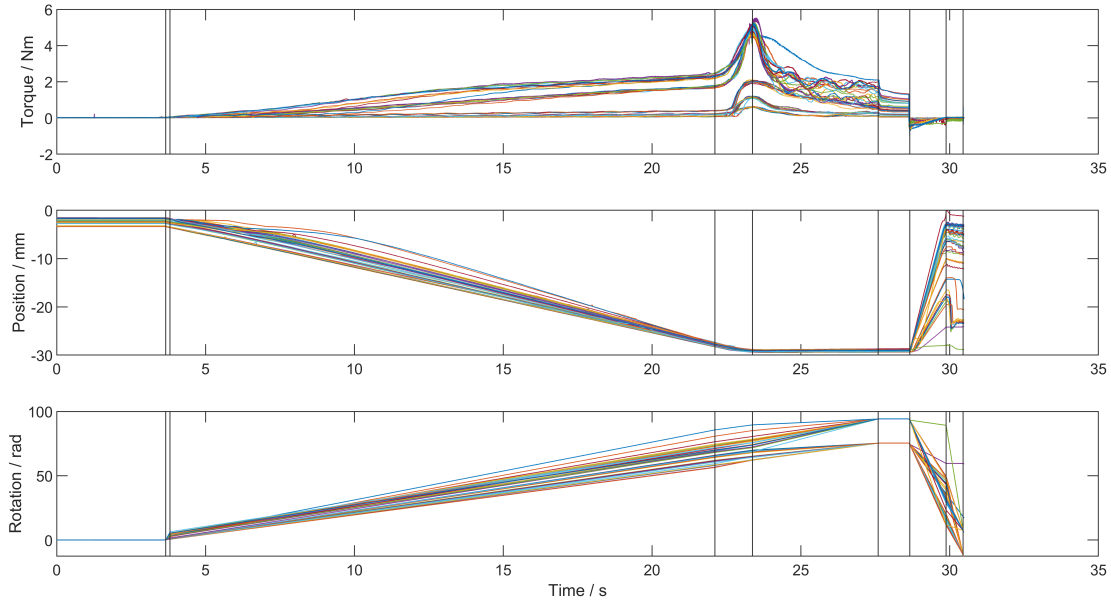

Fig. 4. Result of segmenting all data sets. Times for all datasets have been re-scaled to match the phase transition points from the first set.

percentile and multiple were chosen based on insertion into a relatively hard polyurethane foam, which leads to a stronger torque signal and hence a better SNR. When first tested on data from insertions into softer PU foam, the threshold triggered much earlier in section C, so the values needed to be tuned. If this methodology is applied to data from different materials or collected using different instruments, these thresholds and parameters should be reviewed.

Another limitation of the data collected is that while it measures both angular and linear position, it only measures angular torque, and not linear force. This is mitigated by the use of a 2 kg counterweight to provide a consistent axial force, however for the denser PU foam materials used, additional axial force was required (by pushing on the back of the motor) in order to properly engage the threads with the hole. For the current testing, this variable is not particularly important, however there is some interest in understand the effects of axial force on the initial screw engagement, which was previously explored in Wilkie et al.[15]. Axial force measurement could be achieved by replacing the sample clamp (H in Fig. 1) with one that includes a force sensor; although this would only provide measurement, not actuation. Another alternative could be to use an off-the-shelf linear-torsion test stand such as the Instron ElectroPuls E3000.

The detection of the tightening phase (C-D transition) relies on detecting an increase in the time derivative of the torque. This is similar to the methodology used in Thomas et al. [16]. However, in Thomas et al. [16], this increase is directly used to stop screw insertion, while here is is simply used to determine when the normal insertion phase finishes. The approach from Thomas et al. [16] is effective at preventing stripping, but does not necessarily guarantee an appropriate minimum torque; while the usage here is simply as a pre-processing for a separate model-based method that will try to ensure optimal torquing (not too tight or loose).

Once the preprocessed data presented in this paper is used to validate the previously-presented model-based approach, in addition to other required validation, the model may be used for automated torque limit identification. In a clinical setting, a-priori data about the hole size and screw type would be needed, however the method should be able to automatically determine the appropriate torque based on the torque signal from the specific kind of bone present.

V. Conclusions

A procedure for pre-processing and segmenting screw-insertion test data was developed and implemented with MATLAB. This was tested on 50 sets of data over 5 different densities of polyurethane foam. The segmentation was checked for all datasets and was shown to work reliably under the conditions used. This will be the basis for further processing of this data to validate a system for automated bone-screw torque limit determination.

It should be noted that the thresholds and parameters used for the segmentation may require modification for different test conditions.

This segmented data can be used to validate the previously-presented model-based method, and this will serve as an important step towards potential clinical used. In this setting it may provide more objective torque recommendations for bone screws, potentially improving patient outcomes.

References

[1] M. Evans, M. Spencer, Q. Wang, S. H. White, and J. L. Cunningham, "Design and testing of external fixator bone screws," *Journal of Biomedical Engineering*, vol. 12, no. 6, pp. 457–462, Nov. 1990.

[2] A. Feroz Dinah, S. C. Mears, T. A. Knight, S. P. Soin, J. T. Campbell, and S. M. Belkoff, "Inadvertent Screw Stripping During Ankle Fracture Fixation in Elderly Bone," *Geriatr Orthop Surg Rehabil*, vol. 2, no. 3, pp. 86–89, May 2011.

[3] M. J. Stoesz, P. A. Gustafson, B. V. Patel, J. R. Jastifer, and J. L. Chess, "Surgeon Perception of Cancellous Screw Fixation," *Journal of Orthopaedic Trauma*, vol. 28, no. 1, p. e1, Jan. 2014.

[4] J. Wilkie, P. D. Docherty, and K. Möller, "Developments in Modelling Bone Screwing," *Current Directions in Biomedical Engineering*, vol. 6, no. 3, pp. 111–114, Sep. 2020.

[5] J. Wilkie, P. D. Docherty, T. Stieglitz, and K. Möller, "Geometric Generalization of Self Tapping Screw Insertion Model," in *2021 43rd Annual International Conference of the IEEE Engineering in Medicine Biology Society (EMBC)*, Nov. 2021, pp. 4387–4339.

[6] J. Wilkie, P. D. Docherty, and K. Möller, "Stripping Torque Model for Bone Screws," *IFAC-PapersOnLine*, vol. 54, no. 15, pp. 442–447, Jan. 2021.

[7] J. Wilkie, P. D. Docherty, T. Stieglitz, and K. Möller, "Quantifying Accuracy of Self-Tapping Screw Models," in *2021 43rd Annual International Conference of the IEEE Engineering in Medicine Biology Society (EMBC)*, Nov. 2021, pp. 4391–4394.

[8] International Organization for Standardization, "ISO 5835:1991(en), Implants for surgery — Metal bone screws with hexagonal drive connection, spherical under-surface of head, asymmetrical thread — Dimensions," https://www.iso.org/obp/ui/#iso:std:iso:5835:ed-1:v1:en, 1991.

[9] K. L. Calvert, K. P. Trumble, T. J. Webster, and L. A. Kirkpatrick, "Characterization of commercial rigid polyurethane foams used as bone analogs for implant testing," *J Mater Sci Mater Med*, vol. 21, no. 5, pp. 1453–1461, May 2010.

[10] "Top Biomechanical Products & Materials Provider for Testing & Validation," https://www.sawbones.com/biomechanical-product-info.

[11] "SYNBONE - Generic blocks, foams, rods for biomechanical testing," https://www.synbone.com/products/biomechanics-generics/.

[12] Sika Deutschland GmbH, "SikaBlock M600 Vorläufiges Produktdaten-blatt," Nov. 2014.

[13] O. Cornu, X. Banse, P. L. Docquier, S. Luyckx, and C. Delloye, "Effect of freeze-drying and gamma irradiation on the mechanical properties of human cancellous bone," *Journal of Orthopaedic Research*, vol. 18, no. 3, pp. 426–431, 2000.

[14] C. M. Schoenfeld, E. P. Lautenschlager, and P. R. Meyer, "Mechanical properties of human cancellous bone in the femoral head," *Med. & biol. Engng.*, vol. 12, no. 3, pp. 313–317, May 1974.

[15] J. Wilkie, G. Rauter, and K. Möller, "Initial engagement and axial force model for self-tapping bone screws," *Current Directions in Biomedical Engineering*, vol. 8, no. 2, pp. 753–756, Sep. 2022.

[16] R. L. Thomas, K. Bouazza-Marouf, and G. J. S. Taylor, "Automated surgical screwdriver: Automated screw placement," *Proc Inst Mech Eng H*, vol. 222, no. 5, pp. 817–827, May 2008.